STRUCTURE-BASED DESIGN OF PROTEASE INHIBITORS

Acta Cryst. (1995). D**51**, 550–559

Active-Site Mimetic Inhibition of Thrombin

BY I. I. MATHEWS AND A. TULINSKY*

Department of Chemistry, Michigan State University, East Lansing, MI 48824, *USA*

(*Received* 24 *April* 1994; *accepted* 14 *November* 1994)

Abstract

The structures of two mimetic inhibitor complexes of human α-thrombin have been determined by X-ray crystallography. One mimics a β-turn with a bicyclic ring system; the other mimics two different active-site binding modes. The β-turn mimetic is used to approximate a turn found in the conformation of fibrinopeptide A, which is catalytically released by thrombin in the activation of fibrinogen to fibrin. The binding of the second mimetic is a hybrid between normal substrate and the abnormal binding of the potent natural leech inhibitor hirudin. The binding of the β-turn mimetic is tenuous, because it is like a substrate, while that of the substrate–hirudin hybrid is that of a tenacious inhibitor (which it is). Structurally retrospect modifications for rational design and improvement of both mimetic inhibitors are proposed.

Introduction

One of the most important functions of thrombin is to convert fibrinogen to fibrin. Fibrin is the major component of a blood clot and is responsible for mechanically encapsulating platelets and a number of plasma proteins with a network of fibers that blocks the flow of blood from a punctured or severed blood vessel. Fibrinogen is a disulfide-linked dimer of trimers (three peptide chains with $A\alpha, B\beta, \gamma$ stoichiometry) (Doolittle, 1984). Fibrin assembly begins with the cleavage of two $A\alpha$ chains by thrombin at Arg16-Gly17 with the subsequent release of two molecules of fibrinopeptide A (FPA, Fig. 1) (Blomback, 1967). The FPA deficient fibrinogen is the fibrin monomer that polymerizes to fibrin protofibrils. The second stage of fibrin assembly involves lateral association of protofibrils to form fibers. This stage is accompanied by thrombin cleavage of $B\beta$ chains at Arg14-Gly15 with the release of FPB. The resulting loosely linked network is stabilized by the formation of covalent end-to-end antiparallel bonds between the C terminals of adjacent γ-chains (Chen & Doolittle, 1970). The fibrin structure is additionally covalently stabilized by factor XIIIa, which introduces cross-linking chemical bonds between ε-amino groups of lysine residues and side chains of glutamines. In the activation process of fibrinogen, thrombin exhibits a remarkable specificity in the removal of FPA and FPB by the selective cleavage of only two Arg–Gly bonds out of the 181 Arg/Lys–amino acid peptide bonds in fibrinogen (Blomback, 1967). This is accomplished with a fibrinogen recognition exosite that is distinct from the active site but is generally operative in concert with it.

From the amino-acid sequences of fibrinogen of many species, a portion of the sequence is found to be highly conserved, which led to the proposal that Phe8 at the *P*9 position of the $A\alpha$ chain is essential for normal thrombin response (Blomback, 1967). Scheraga and coworkers have used several methods of investigating the interaction of thrombin with fibrinogen to confirm the conjecture (Scheraga, 1986). These studies showed that the N-terminal six residues of FPA do not interact with thrombin whereas Asp7-Phe8 influence the effectiveness of the binding of synthetic peptide substrates to thrombin. This led to another proposal that FPA has a bent conformation bringing Phe8 close to Arg16 (Blomback, Olsson, Svendsen & Aberg, 1969; Rae & Scheraga, 1979). Later NMR results showed that Asp7–Leu9 and Val15-Arg16 are involved in the interaction with thrombin, Phe8–Ala10 are in a helical segment and that a β-bend is present centered at Glu11–Gly13 (Ni, Meinwald, Vasquez & Scheraga, 1989).

The foregoing generalities led us to investigate the structure of the human FPA–human thrombin complex by X-ray crystallography (unpublished results of this laboratory). An attempt to produce a ternary complex of FPA with fibrinogen exosite hirugen-inhibited thrombin (Fig. 1) led to crystals that were identical to the hirugen–thrombin complex (Skrzypczak-Jankun *et al.*, 1991). Crystallization of α-thrombin in the presence of the divalent inhibitor hirulog2 (Fig. 1) also produced the hirugen–thrombin structure with nothing bound in the active site. Since hirulog2, like hirulog1 (Fig. 1), is a poor substrate for thrombin ($k_{cat} \simeq \text{min}^{-1}$) (Skrzypczak-Jankun *et al.*, 1991; Witting, Bourdon, Brezniak, Maraganore & Fenton, 1992), it was cleaved at the Arg–Pro bond with the subsequent release of FPA. An attempt was also made to simply crystallize a binary FPA human α-thrombin complex. Although diffraction-quality crystals were obtained, they proved to be those

* To whom correspondence should be addressed.

of the autolysis product γ-thrombin (Rydel *et al.*, 1994). All the foregoing is in agreement with the relatively weak binding constant of FPA ($K_m = 310\ \mu M$) for thrombin (Marsh, Meinwald, Thannhauser & Scheraga, 1983). The FPA–hirugen–thrombin ternary complex probably did not form in sufficient quantity because of this and in an attempt to prepare the binary FPA–thrombin complex, α-thrombin was not completely inactivated by FPA to prevent autolysis to the less active γ-thrombin form during the time required for crystallization (days to weeks).

The structures of a ternary human α-thrombin complex of hirugen with the covalently linked *N*-acetyl chloromethylketone of FPA (Stubbs *et al.*, 1992) as well as that of human FPA bound to bovine thrombin (Martin *et al.*, 1992) have been determined. In the latter structure, there are three thrombin molecules in the asymmetric unit, one of which is most likely to be the ε-thrombin autolysis product with a cleavage at Thr149A–Ser149B while the other two appear to be α-thrombin. The FPA was found to bind to each molecule, but due to its weak binding constant, only with an average occupancy of about 60%. Both the FPA and the FPA chloromethylketone thrombin complexes have a turn between Leu9 and Gly12.

The reverse-turn framework was examined by computer graphics modeling (Nakanishi *et al.*, 1992) utilizing a bicyclic β-turn mimetic and by crystallography of its synthetic chloromethylketone peptide (FPAM, Fig. 1*a*) (Wu *et al.*, 1993). The modeling was based on the NMR structure (Ni *et al.*, 1989) and suggested changes in the NMR ψ angles of Val15-Arg16 (no transfer NOE constraints on the orientation of the arginyl side chain) in order to achieve a binding conformation. The crystallographic structure of the FPAM–thrombin complex differed from the FPA–thrombin structures in that the bicyclic β-turn position was at Glu11–Gly13 instead of one residue over toward the N terminus. Here we report further refinement and details of the interaction of FPAM with thrombin, compare its binding with that of the two FPA–bovine thrombin complexes and propose in retrospect modifications in the design of FPAM to mimic the folded structure of FPA more closely.

Another class of distinct synthetic highly specific thrombin inhibitors has evolved, originally based only on the chemical nature of the binding subsites of thrombin. The earliest of these was dansylarginine *N*-(3-ethyl-1,5-pentanediyl) amide (DAPA, Fig. 2*b*) (Okamoto *et al.*, 1976; Hijikata *et al.*, 1976), which was also exploited as a fluoresence probe (Nesheim, Prendergast & Mann, 1979). The binding of members of this class of inhibitors† to thrombin (Banner & Hadvary, 1991; Brandstetter *et al.*, 1992) and trypsin (Matzusaki, Sasaki, Okmura & Umeyama, 1989; Bode, Turk & Sturzebecher, 1990; Turk, Sturzebecher & Bode, 1991) has been studied by crystallography and the trypsin results have been extended to thombin by analogy and molecular modeling (Bode, Turk & Sturzebecher, 1990; Turk, Sturzebecher & Bode, 1991). The bovine thrombin complexes were determined at 2.3 Å resolution using the autolytic ε-thrombin form (Brandstetter *et al.*, 1992) while those involving human thrombin (Banner & Hadvary, 1991) were at lower 3.0 Å resolution. We also report here the structure and binding of the DAPA mimetic inhibitor with human α-thrombin at 2.3 Å resolution, and its relationship to other substrate–inhibitor binding modes at the active center.

Experimental procedures

The preparation and crystallization of the ternary FPAM–thrombin–hirugen crystals has been reported elsewhere (Wu *et al.*, 1993). The DAPA–thrombin–hirugen complex was prepared similarly by adding a tenfold molar excess of DAPA solution to a solution of the hirugen–thrombin complex (Skrzypczak-Jankun *et al.*, 1991). The DAPA–thrombin crystal used for X-ray intensity data collection grew in about two weeks and was about 0.4 × 0.3 × 0.25 mm in size.

The intensity data sets of the FPAM– and DAPA–thrombin crystals were measured with a Siemens X-1000 multiwire area detector with graphite-monochromated Cu$K\alpha$ radiation from a Rigaku RU200 rotating-anode generator. The instrumental conditions and the measurement modes were the same for both crystals (Wu *et al.*, 1993). The crystals are isomorphous with the hirugen–thrombin complex: FPAM–thrombin–hirugen, monoclinic, space group $C2$, four complexes per unit cell, $a = 71.13, b = 72.43, c = 73.00$ Å, $\beta = 101.1°$; DAPA–thrombin–hirugen, $a = 72.08,\ b = 72.55,\ c = 73.84$ Å,

† Abbreviations used for members of this class are: Argatroban, (2*R*,4*R*)-4-methyl-1-[N^{α}-(3-methyl-1,2,3,4-tetrahydro-8-quinolinesulfonyl)-L-arginyl]-2-piperidinecarboxylic acid (also known as MQPA, Argipidine, Novastan® and Slounon®); NAPAP, $N\alpha$-(2-naphthylsulfonyl-glycyl)-DL-*para*-aminophenyl piperidine. For structural formulae, see Brandstetter *et al.* (1992).

	7	10	15	20
FPA(7-20)	Ace- D - F - L - A - E - G - G - G - V - R - G - P - R - V - $NHCH_3$			
Hirugen, [Hirudin (53-64)]			Ace - N - G - D - F - E - E - I - P - E - E - Y*- L	
Hirulog 2	FPA(7-16) - P - G - G - G - G - N - G - D - F - E - E - I - P - E - E - Y - L			
Hirulog 1	d - F - P - R - P - G - G - G - G - N - G - D - F - E - E - I - P - E - E - Y - L			

Fig. 1. Thrombin peptide substrate–inhibitor complexes. The asterisk indicates sulfated tyrosine.

$\beta = 101.4°$. The DAPA complex diffracted X-rays to about 2.3 Å resolution (46320 observations; 14467 independent reflections; R_{merge} on $|F|^2 = 0.039$); the FPAM complex did not scatter quite as far at 2.5 Å resolution (37533 observations; 11675 independent reflections; R_{merge} also 0.039).

Both starting structures (hirugen–thrombin) were refined using restrained least-squares methods with the programs *PROLSQ* or *PROFFT* following similar protocols (Wu *et al.*, 1993). In both cases, the dictionary was modified to introduce proper restraints for the inhibitor. To simplify the dictionary restraints of DAPA, it was treated in three parts (Fig. 2*b*). The *B* and *D* regions were considered as special groups, distance and planar restraints were applied externally in the control file and the groups were excluded from the peptide-chain sequence. The externally applied restraints of both inhibitors are indicated in Fig. 2. Since the Pha1 and Ben groups (Fig. 2*a*) had marginal electron density with breaks and the bicyclic ring was not completely covered with electron density (Wu *et al.*, 1993), both groups and about 50 lower occupancy water molecules were removed from FPAM–thrombin and the structure was additionally refined. The resulting $(2|F_o| - |F_c|)$, $(|F_o| - |F_c|)$ and *OMIT* difference maps showed even poorer indications of the Pha1 and Ben2 substituents, which also extended to include some of the seven-membered ring. Consequently, these regions were withheld from further refinement, which converged at: $R = 0.140$, 179 water molecules with occupancy > 0.5 and $B < 40$ Å^2 and with a $\langle B \rangle = 28$ Å^2 for the thrombin molecule. Although these and other refinement parameters are indistinguishable from those reported previously (Wu *et al.*, 1993), the present structure, which contains less of the FPAM mimetic, is without questionable parts. The refinement of the DAPA complex proceeded uneventfully and in a routine manner converging at: $R = 0.147$, 201 water molecules, also with occupancy > 0.5, $B < 40$ Å^2 and with a $\langle B \rangle = 21$ Å^2, in agreement with the better X-ray scattering of DAPA–thrombin crystals. Both sets of refined coordinates have been deposited with the Protein Data Bank.*

Results and discussion

(i) *FPAM–Thrombin*

Designed conformationally restricted non-peptide β-turn prosthetic units have been attached to the amino terminals of peptides by Kahn and coworkers (Kahn, Wilke, Chen & Fujita, 1988; Kahn *et al.*, 1988; Kahn & Bertenshaw, 1989). In particular, a synthetic 11-membered bicyclic *bis*-lactam ring system (Figs. 2*a* and 2*c*) was made to conformationally mimic type I and type II β-turns. The r.m.s. difference in six atom positions of the two lowest energy, 11-membered ring conformations and idealized β-turns is about 0.7 Å for type II and 1.2 Å for type I (Kahn *et al.*, 1988). Using less rigorous and more realistic β-turn definitions (Lewis,

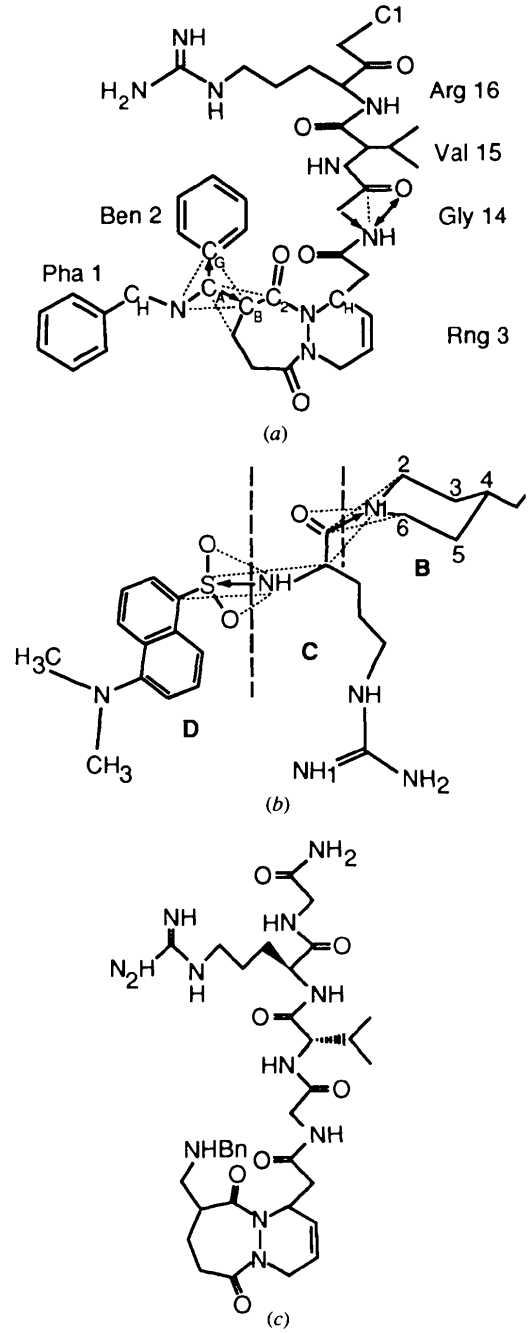

Fig. 2. Mimetic inhibitors of thrombin. (*a*) FPAM, (*b*) DAPA, (*c*) FPAM1. Special restraints applied to non-amino-acid groups during refinement to maintain geometry: arrow, bond distance; dotted, angle distance, double arrow, planar 1,4 distance and NB—B1—B3—B4, B2—B3—B5—NB in DAPA.

* Atomic coordinates have been deposited with the Protein Data Bank, Brookhaven National Laboratory [Reference: 3HAT (FPAM), 1FPC (DAPA)]. Free copies may be obtained through The Managing Editor, International Union of Crystallography, 5 Abbey Square, Chester CH1 2HU, England (Reference: GR0501).

Momany & Scheraga, 1973; Richardson, 1981) reduced the differences significantly. The proposal of a bent conformation for FPA (Scheraga, 1986) and the subsequent NMR report of its position (Ni *et al.*, 1989) led to the design and synthesis of the specific chimeric thrombin substrate FPAM (Nakanishi *et al.*, 1992).

As judged by kinetic competency, the (*R*,*S*) and (*S*,*R*) isomers of FPAM 1 (Fig. 2*c*) closely mimic the thrombin-bound conformation and compare well with those of FPA (8–18) (Nakanishi *et al.*, 1992). The mimetic substrate is better than the undecapeptide and is comparable to the 51-residue cyanogen bromide cleavage fragment of the fibrinogen *Aα* chain (Marsh *et al.*, 1983). The hybrid mimetic structure can be readily docked computationally to the thrombin active site using the structure of bovine pancreatic trypsin inhibitor (BPTI) bound to trypsin (Huber *et al.*, 1974) as a template. The modeling information was used to design and synthesize a FPAM (Fig. 2*a*) diastereoisomer of unknown stereochemistry. This substrate-derived conformationally restricted hybrid mimetic inhibitor of thrombin has a $K_{app}/I = 4.4 \times 10^4\, M^{-1}\,\text{min}^{-1}$.* By comparison, the exceptionally potent thrombin inhibitor D-Phe-Pro-Arg chloromethyl ketone (PPACK) has $K_{app}/I = 1.6 \times 10^7\, \text{M}^{-1}\,\text{min}^{-1}$ (Nakanishi *et al.*, 1992).

The manner in which FPAM fills the active site of thrombin is shown in Fig. 3. In the complex, His57 NE is alkylated while the carbonyl group of Arg16 of FPAM forms an intermediate hemiketal in the catalytic site with Ser195 OG and the interactions effectively turn off the catalytic machinery of thrombin. The *S*1 specificity site of the complex is occupied with the arginyl group of Arg16 of FPAM (Fig. 3*b*), similar to other active-site-directed thrombin complexes, with the guanidinium group forming a doubly hydrogen bonded salt bridge to the carboxylate of Asp189. The side group of Val15 is buried in the hydrophobic *S*2 apolar subsite (Fig. 3*b*), like the proline in PPACK–thrombin (Fig. 4), making close contacts with Tyr60A and Trp60D of the 60 insertion loop and the side chain of Leu99. The Gly14–Arg16 stretch makes an antiparallel two-hydrogen-bonded *β*-strand interaction similar to PPACK–thrombin that appears to also be important in positioning the bicyclic ring of FPAM, which occupies the same region as D-Phe of PPACK (Fig. 4). The bicyclic *β*-bend is surrounded by Leu99, Ile174, Trp215 and Val15 of FPAM (Fig. 3 and 4). The new electron density, however, deteriorates for the seven-membered ring (is below 0.8σ) and is not well defined. This also includes

* The quantity K_{app}/I is used because the kinetics were measured by competition with a substrate rather than by direct analysis. In the one substrate case, the Michaelis–Menten parameters are treated as constants, whereas in the present case, they are 'apparent values' and constant only if the concentration of the other substrate is constant.

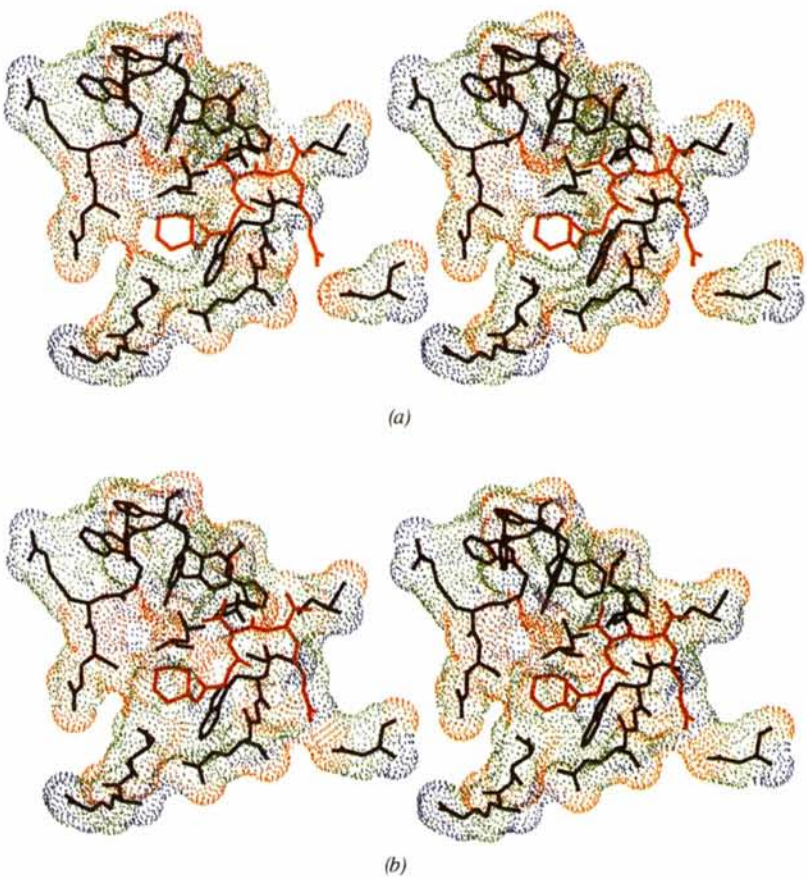

Fig. 3. Stereoview of FPAM bound in the active site of thrombin. FPAM is red; Connolly dot surface of FPAM omitted in (*a*) and superimposed in (*b*). Thrombin residues as in Figs. 4 and 5.

the Pha1 and Ben aromatic substituents of the ring that have to extend outward toward the surface of the thrombin molecule. The six-membered azohexene (Fig. 2*a*) can only assume three undistorted conformations (chair, boat and envelope) and appears to be in the boat form. The seven-membered ring system is much more flexible and can assume a large number of ring conformations through free bond rotations. This part of the inhibitor is flexibly disordered among a number of these different conformational positions. Further evidence of the disorder is given by the $(|F_o| - |F_c|)$ density being more noisy than average for the region even though there is no corresponding density in the $(2|F_o| - |F_c|)$ map. However, there is density in the latter attached to Ile174 CD1 and a significant positive peak in the difference map corresponding to it that may represent two alternate conformations of the Ile174 reflecting the flexibility of the seven-membered ring and its substituents. The exposure of the Pha1 and Ben groups to solvent may be an important overall contributing factor to the ring flexibility. Thus, the former description of the bound conformations of these rings are only marignally reliable (Wu *et al.*, 1993).

The average value of the thermal parameter of FPAM is about 49 Å^2 while that of the thrombin molecule is 28 Å^2. The *B* values of the Val-Arg peptide of FPAM, its covalent link to His57 and the hemiketal are normal but increase at the glycine linker and for the azocyclohexene ring of the bicyclic β-turn mimetic. Similar high *B* values have been observed in other thrombin complexes where large differences were attributed to imprecision in the positioning of inhibitor (Rydel, Tulinsky, Bode & Huber, 1991; Mathews *et al.*, 1994); the activation domain of prethrombin 2, the immediate inactive precursor of α-thrombin, also has large *B* differences for similar reasons (Vijayalakshmi, Padmanabhan, Mann & Tulinsky, 1995). Another source of high *B* values can be partial occupancy, as was the case in the FPA–bovine thrombin complex (Martin *et al.*, 1992). With FPAM–thrombin, however, the covalent bond should lead to complete inhibition or nearly so.

The structures of FPA in the human FPA bovine thrombin complex (Martin *et al.*, 1992) and the FPA chloromethyl ketone–thrombin derivative (Stubbs *et al.*, 1992) are practically the same (r.m.s. $\Delta = 0.6$ Å and only 0.3 Å if the side groups of Leu9 and Glu11 are not included). The φ, ψ conformational angles of the *P*1–*P*2–*P*3 residues of both and those of FPAM agree closely as well as with the conformation of PPACK in PPACK–thrombin and Pro13–Lys15 of BPTI in its complex with trypsin (Huber *et al.*, 1974). This can be seen from Fig. 5, which compares the structure of the FPAM–thrombin and the FPA–bovine thrombin complex. The structure of the FPAM complex does not correspond to that of FPA in one important respect: a one-residue peptide insertion following the bicyclic ring (C-terminal to the ring) would place the β-turn of the mimetic more optimally with respect to the turn in FPA. The bicyclic turn does not correspond to the turn of FPA because its design (between Glu11 and Gly13) was based on the position

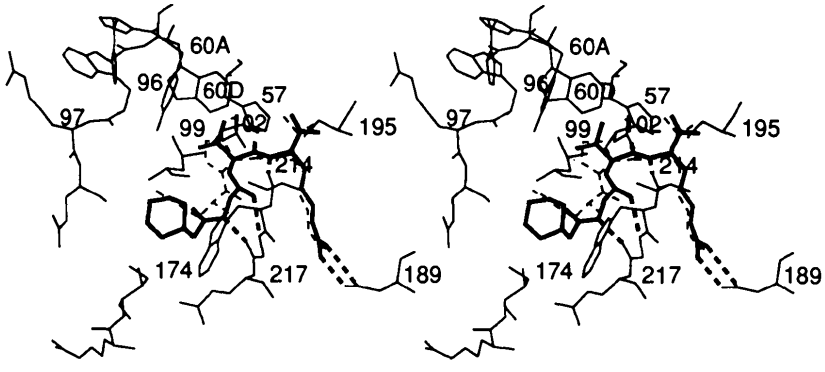

Fig. 4. Stereoview of the comparison of the binding of FPAM and PPACK in the active site of thrombin. FPAM, in bold; PPACK in broken; thrombin in solid lines; hydrogen bonds in bold broken lines.

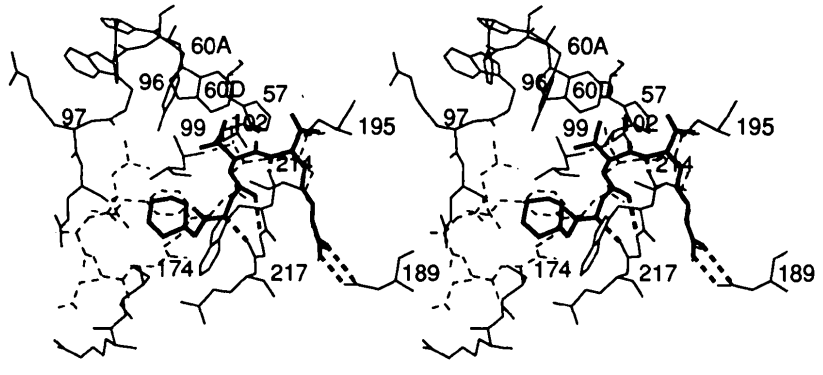

Fig. 5. Stereoview of the comparison of the binding of FPAM and FPA in the active site of human thrombin. FPAM in bold; FPA in broken; thrombin in solid lines; hydrogen bonds in bold broken lines.

proposed from NMR measurements, which differs by one residue from the crystallographic results. The NMR results, however, correctly assign a helical conformation for the N-terminal of the FPA molecule in agreement with the crystalline complexes. The shortcomings of FPAM with respect to FPA can be accommodated by some additional design features (insertion of a peptide between Gly14 and the bicyclic turn and extending the benzylate peptide link to mimic the Phe8, Val15 interaction, Fig. 6*a*). An even better conformed, bound-FPA mimetic can be approximated by inserting the tri- or tetrapeptide of FPA (Asp-Phe-Leu-Ala) to preceed the β-turn bicyclic mimetic (Fig. 6*b*) in order to possibly approximate the N-terminal helical turn.

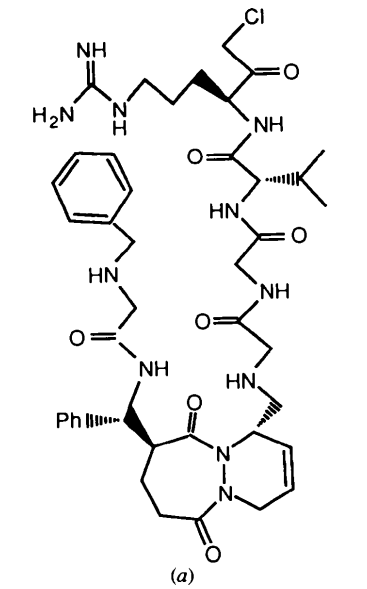

(*a*)

(*b*)

Fig. 6. Possible design changes to improve the binding of bicyclic β-turn peptide mimetics. (*a*) Extension of FPAM design, (*b*) extension mimicking with the FPA sequence.

The active site of thrombin is capable of and actually binds peptides in three distinct modes (Tulinsky & Qiu, 1993): (1) like FPA substrate, (2) N-terminal hirudin-like (Rydel *et al.*, 1990; Grutter *et al.*, 1990; Rydel, Tulinsky, Bode & Huber, 1991) and (3) Argatroban or DAPA-like (Banner & Hadvary, 1991; Brandstetter *et al.*, 1992). The binding of FPAM is pseudo-FPA substrate differing from the latter in the position of the β-turn. This is yet another example of the dichotomy that exists between specificity and alternate modes of achieving it and is all the more noteworthy in that it also extends to the other binding exosites (fibrinogen, heparin) of thrombin (Tulinsky & Qiu, 1993).

(ii) *DAPA*-Thrombin

The inhibitor DAPA is highly specific and potent for thrombin. The selectivity coupled with the increase of fluorescence properties of the dansyl group upon binding and its lack of inhibition of factor Xa made it a very useful probe for monitoring thrombin formation during the activation of prothrombin (Nesheim *et al.*, 1979). Although not susceptible to hydrolysis catalyzed by thrombin, it competively inhibits thrombin-catalyzed hydrolysis of either synthetic substrates or fibrinogen with a K_i of about $10^{-7}M$ with a high degree of selectivity. Many of the unique properties of DAPA appear to derive from the 4-ethylpiperidine moiety of the molecule, which confers both greater potency and specificity compared with other ester and amide derivatives (Okamoto *et al.*, 1976).

Inhibitor binding by proteins or enzymes is a complex thermodynamic process driven by both energetic and entropic changes. The change of free energy of inhibitor binding, resulting from the addition or deletion of functional groups, arises from energy differences associated with different protein contacts, conformational entropy changes to the protein and inhibitor and to differences in the solvation/desolvation thermodynamics of inhibitor and protein (Beveridge & DiCapua, 1989). The major interactions of active-site inhibitors and thrombin take place through the *S*1 specificity site, hydrogen bonding with the Ser214–Gly216 stretch and hydrophobic interactions with the apolar *S*2 subsite and the indole ring of Trp215. A significant finding that has emerged from the structures of many different active-site inhibitors is that thrombin can accommodate different inhibitor types in different ways (Tulinsky & Qiu, 1993). DAPA, and members of its class of inhibitors, associates with thrombin in one of these different binding modes.

The DAPA molecule is clearly defined in the electron density and it binds to thrombin in a conformationally compact structure (Fig. 7). Overall, the interactions are also pseudo-substrate-like compared to FPA and PPACK and are similar to those of the thrombin complexes of Argatroban, NAPAP and 4-TAPAP (Brandstetter *et al.*,

1992). The backbone of DAPA runs antiparallel to Ser214–Gly216, but not as a true β-strand, forming only one good hydrogen bond, which is between the N atom of the arginine of DAPA and the carbonyl group of Gly216 (2.8 Å) (Fig. 8); an adjacent interaction of the carbonyl of the arginine and the N atom of Gly216 appears to be a marginal hydrogen bond (3.0 Å, ∠C—O—N, 142°). In both the DAPA- and PPACK–thrombin complexes, however, the carbonyl displaces O_w580 of the hirugen–thombin complex (Vijayalakshmi *et al.*, 1995). Moreover, the arginyl side chain of DAPA enters the *S*1 specificity site about 4.1 Å displaced from the position observed with normal substrates (about one residue) and from a different direction (Fig. 8). As a result, the guanidinium group does not approach the carboxylate of Asp189 head-on and forms a non- or weakly hydrogen-bonded salt bridge through only one of its N atoms (NH1) instead of the usual doubly hydrogen-bonded ion pair (Fig. 8). The NH1 is about equispaced from the two carboxylate O atoms (Table 1). The C-terminal piperidine ring, formally at the *P*1′ position of substrate, is in a chair conformation occupying the apolar *S*2 subsite and is squeezed between the dansyl naphthyl group and the imidazole ring of His57 of thrombin while the 4-ethyl group of the piperidine is close to the side chains of Tyr60A and Trp60D (Fig. 8). The naphthyl of DAPA characteristically occupies the aromatic *S*3-binding site (Bode, Turk & Karshikov, 1992) and is

Table 1. *Polar and bridging interactions of DAPA with thrombin*

DAPA/O_w	Thrombin/O_w	Distance (Å)	Comment
Arg371 NH1	Asp189 OD1	3.3	Ion pair
Arg371 NH1	Asp189 OD2	3.2	Ion pair
Arg371 NH2	O_w404	3.4	Hydrogen-bonded solvent bridge (?)
O_w404	Phe227 O	3.1	
Arg371 NH2	O_w454	2.7	Hydrogen-bonded solvent bridge
O_w454	Ser195 OG	2.7	
Dan370 SO1	O_w564	3.4	Hydrogen-bonded solvent bridge (?)
O_w564	Glu192 OE2	2.7	

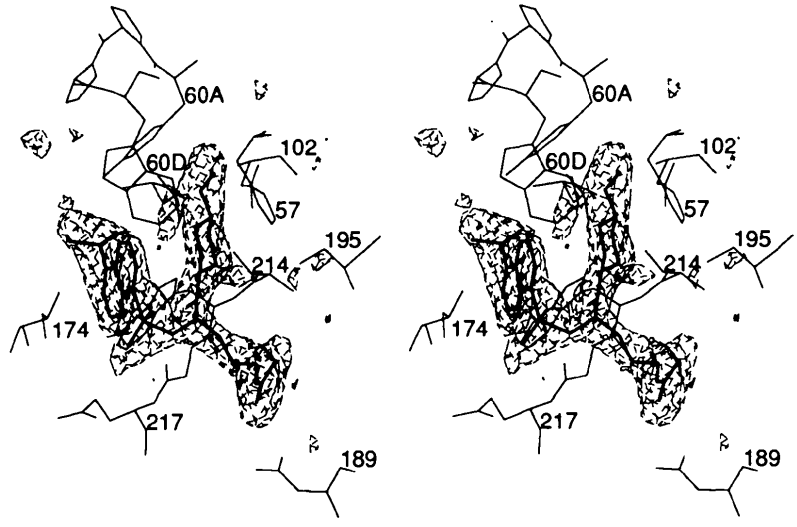

Fig. 7. Stereoview of the *OMIT* difference electron density of the DAPA molecule. DAPA in bold; thrombin in thin lines; contoured at 2.0σ.

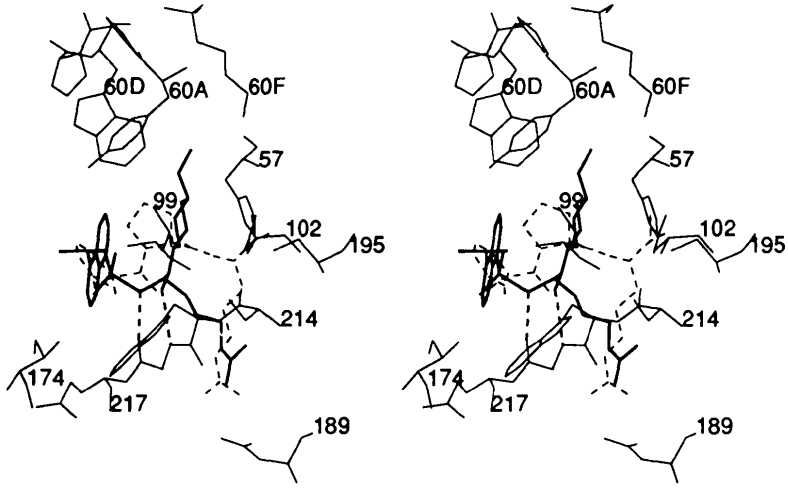

Fig. 8. Stereoview of the comparison of the binding of DAPA and PPACK in the active site of thrombin. DAPA in bold; thrombin, solid lines; PPACK broken; hydrogen bonds broken bold lines.

almost perpendicular to the indole ring of Trp215. Both O atoms of the dansyl sulfonyl are directed away from the thrombin surface and are in contact with water molecules. One of the water molecules (O_w564) mediates an interaction between a sulfonyl O atom and Glu192 of thrombin. Other bridging inhibitor–thrombin interactions are summarized in Table 1. The NH2 of the arginine side chain of DAPA bridges to Ser195 OG of the catalytic triad through O_w454 and to Phe227 O through O_w404.

An important distinction between the binding of DAPA and PPACK is that the former satisfies the *S*2–*S*3 subsites with groups that are 1,3 in position to the arginine while PPACK and substrate achieve it with 2,3 side chains. In this respect, then, DAPA is similar in binding to the Ile1–Tyr3 N-terminal of hirudin (Fig. 9) (Rydel *et al.*, 1991). The principal difference between the two is that the chain direction of DAPA runs like substrate and is not reversed to form a parallel β-strand as in hirudin. The correspondence in the binding of the two is strikingly close, even to the positions of the C_α atoms of the arginyl of DAPA and Thr2 of hirudin ($\Delta = 0.7$ Å) (Fig. 9).

The structure of DAPA bound to thrombin can be considered as a hybrid between pseudo-substrate and the N-terminal of hirudin. The action of DAPA, however, can be thought of a classic example of 'working for the wrong reasons'. By itself, it appears to mimic the *P*2–*P*1–*P*1′ positions of substrate. Although the *P*1 position occupies the specificity site in an approximate manner, in the thrombin complex, *P*1′ is in *S*2 while *P*2 occupies the *S*3 site. Yet, this class of inhibitors is so selective for thrombin that Argatroban is marketed as an antithrombotic drug in Japan under the registered trademarks Novastan® and Slounon®. All the more impressive is the fact that DAPA was designed without the benefit of three-dimensional structure-based knowledge of the receptor. This may have been timely in that, otherwise, the DAPA structure may not have been conceived as it was, using inferences from natural substrates and inhibitors along with screening methods assisted by substrate–activity relationships.

The ability of thrombin to bind structurally different inhibitors in the active site appears to be related to some degree to the displacement of conserved water molecules of the region. In the structure of the hirugen–thrombin complex where the active site is unoccupied, there are about 15 water molecules in the vicinity (Vijayalakshmi *et al.*, 1995). All five water molecules in the *S*1 specificity site also have counterparts in complexes of thrombin with hirudin and the MDL-28050 peptide where the active site is also not inhibited (Qiu, Yin, Padmanabhan, Krstenansky & Tulinsky, 1993). Three of these waters are displaced by an arginyl group upon binding PPACK or DAPA (O_w477, O_w555, O_w561). The piperidine moiety of DAPA displaces two waters of hirugen–thrombin (O_w641, O_w642). One of the bridging water molecules of DAPA–thrombin (O_w404) (Table 1) is conserved in most thrombin active-site complexes while the other (O_w454) is a new interaction in DAPA–thrombin. To complete the inhibitor–solvent interaction, DAPA itself is surrounded by seven new water molecules in the thrombin complex; in PPACK–thrombin six new water molecules interact with PPACK (Vijayalakshmi *et al.*, 1995). A principal source of all the unique interactions of DAPA is the binding of the *P*1′ group of DAPA in the *S*2 apolar subsite of thrombin. The drastically different positioning of the C_α atom of the arginyl residue of DAPA, compared to normal substrate (Fig. 8), is also the result of the incongruent binding of the *P*1′ piperidine ring.

The presence of charged side chains, potential donor/acceptor hydrogen-bonding groups and water molecules of thrombin near the piperidine and dansyl rings of DAPA in the complex offer the possibility of additional

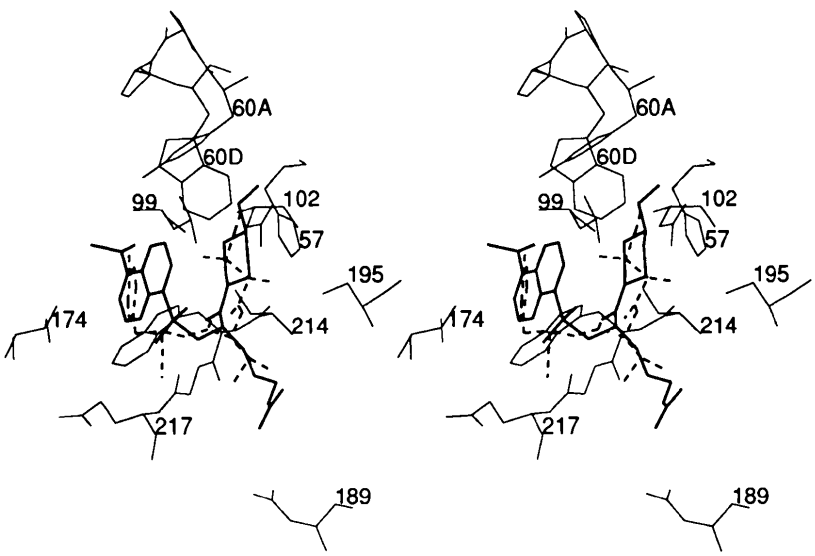

Fig. 9. Stereoview of the comparison of the binding of DAPA and the N-terminal of hirudin in the active site of thrombin. DAPA in bold; N-terminal Ile1-Thr2-Tyr3 of hirudin broken; thombin solid lines.

stabilizing influences through suitable substitutions. Modeling with various substituents on the piperidine indicates that the axial position of B2 could be an important determinant in enhancing binding (Fig. 2*b*). This is corroborated by the structure of the Argatroban–thrombin complex where there is a carboxylate at this position that can interact with His57 (Brandstetter *et al.*, 1992). Insertion of a methylene between the ring and the carboxyl group may even increase the interaction. In doing so, the carboxylate group would displace two more water molecules from the active site (O_w467, O_w513) of the DAPA–thrombin complex. The carboxylate enhancement in Argatroban is that much more impressive since there are five negative charges in the active-site region (Glu91A, Asp102, Glu146, Glu192, Glu217). With the methylene (or longer) extension, the carboxylate could reach the oxyanion hole involving Gly193 and Ser195. Precedence for such an interaction has been set by the structure determination of a thrombin platelet-receptor peptide–thrombin complex where an aspartate of the peptide occupies this position in a non-productive binding mode (Mathews *et al.*, 1994). Another viable alteration would be to replace the carboxylate and mimic the N-terminal of hirudin where the α-amino group hydrogen bonds with Ser195 OG. Such a change in electrical polarity might also be well received by the already highly electronegative active-site region.

Substitution of an ethyl or an isopropyl group on the B3 or B5 position of the piperidine (Fig. 2*b*) would appear to serve to fill the *S*2 site of thrombin more fully, and placement of a negatively charged carboxylate on the 4-ethyl group could produce an ion pair with Lys60 F of thrombin (Figs. 8 and 9). A bulkier substituent on the naphthyl ring would also seem to pack the *S*3 aryl site more fully. This approximation is partially attained by Argatroban, which has a tetrahydronaphthyl ring. Although the alternatives for rational improvement are many, in the case of Argatroban-like structures, they are, however, more like gilding a lily rather than growing it.

This work was supported by NIH grant HL 43229. We would like to thank Dr T.-P. Wu for carrying out the initial crystallographic work on the FPAM complex; we would also like to thank the following for providing us with precious materials: John Fenton (thrombin), Mike Kahn (FPAM), Ken Mann (DAPA), John Maraganore (hirugen, hirulog1 and hirulog2) and Harold Scheraga [FPA(7-20)]; in addition, thanks are due to Wolfram Bode and Brian Edwards for providing us with the coordinates of the FPA–thrombin complexes and Dr Pappan Padmanabhan for help throughout the work.

References

Banner, D. W. & Hadvary, P. (1991). *J. Biol. Chem.* **266**, 20085–20093.

Beveridge, D. L. & DiCapua, F. M. (1989). *Annu. Rev. Biophys. Chem.* **18**, 431–492.

Blomback, B. (1967). *Blood Clotting Enzymology*, edited by W. H. Seegers, pp. 143–215. New York: Academic Press.

Blomback, B., Blomback, M., Olsson, P., Svendsen, L. & Aberg, G. (1969). *Scand. J. Clin. Lab. Invest.* **24**, 59–64.

Bode, W., Turk, D. & Karshikov, A. (1992). *Protein Sci.* **1**, 426–471.

Bode, W., Turk, D. & Sturzebecher, J. (1990). *Eur. J. Biochem.* **193**, 175–182.

Brandstetter, H., Turk, D., Hoeffken, H. W., Grosse, D., Sturzebecher, J., Martin, P. D., Edwards, B. F. P. & Bode, W. (1992). *J. Mol. Biol.* **226**, 1085–1099.

Chen, R. & Doolittle, R. F. (1970). *Proc. Natl Acad. Sci. USA*, **66**, 472–479.

Doolittle, R. F. (1984). *Annu. Rev. Biochem.* **53**, 195–229.

Grutter, M. G., Priestle, J. P., Rahuel, J., Grossenbacher, H., Bode, W., Hofsteenge, J. & Stone, S. R. (1990). *EMBO J.* **9**, 2361–2365.

Hijikata, A., Okamoto, S., Mori, E., Kinjo, K., Kikumoto, R., Tonomura, S., Tamao, Y. & Hara, H. (1976). *Thromb. Res. Suppl.* 2, **8**, 83–89.

Huber, R., Kukla, D., Bode, W., Schwager, P., Bartels, K., Diesenhofer, J. & Steigeman, W. (1974). *J. Mol. Biol.* **89**, 73–101.

Kahn, M. & Bertenshaw, S. (1989). *Tetrahedron Lett.* **30**, 2317–2320.

Kahn, M., Wilke, S., Chen, B. & Fujita, K. (1988). *J. Am. Chem. Soc.* **110**, 1638–1639.

Kahn, M., Wilke, S., Chen, B., Fujuita, K., Lee, Y.-H. & Johnson, M. E. (1988). *J. Mol. Recog.* **1**, 75–79.

Lewis, P. N., Momany, F. A. & Scheraga, H. A. (1973). *Biochem. Biophys. Acta*, **303**, 211-229.

Marsh, H. C., Meinwald, Y. C., Thannhauser, T. W. & Scheraga, H. A. (1983). *Biochemistry*, **22**, 4170–4174.

Martin, P. D., Robertson, W., Turk, D., Huber, R., Bode, W. & Edwards, B. F. P. (1992). *J. Biol. Chem.* **267**, 7911–7920.

Mathews, I. I., Padmanabhan, K. P., Ganesh, V., Tulinsky, A., Isshii, M., Chen, J., Turck, C. W. & Coughlin, S. R. (1994). *Biochemistry*, **33**, 3266–3279.

Matsuzaki, T., Sasaki, C., Okumura, C. & Umeyama, H. (1989). *J. Biochem. (Tokyo)*, **105**, 949–952.

Nakanishi, H., Chrusciel, R. A., Shen, R., Bertenshaw, S., Johnson, M. E., Rydel, T. J., Tulinsky, A. & Kahn, M. (1992). *Proc. Natl Acad. Sci. USA*, **89**, 1705–1709.

Nesheim, M. E., Prendergast, F. G. & Mann, K. G. (1979). *Biochemistry*, **18**, 996–1003.

Ni, F., Meinwald, Y. C., Vasquez, M. & Scheraga, H. A. (1989). *Biochemistry*, **28**, 30.

Okamoto, S., Hijikata, A., Ikezawa, K., Kinjo, K., Kikumoto, R., Tonomura, S. & Tamao, Y. (1976). *Thromb. Res. Suppl.* 2, **8**, 77–82.

Qiu, X., Yin, M., Padmanabhan, K. P., Krstenansky, J. L. & Tulinsky, A. (1993). *J. Biol. Chem.* **268**, 20318–20326.

Rae, I. D. & Scheraga, H. A. (1979). *Int. J. Pept. Protein Res.* **13**, 304–314.

Richardson, J. S. (1981). *Ad. Protein Chem.* **34**, 167–339.

Rydel, T. J., Ravichandran, K. G., Tulinsky, A., Bode, W., Huber, R., Roitsch, C. & Fenton, J. W. II (1990). *Science*, **249**, 277–280.

Rydel, T. J., Tulinsky, A., Bode, W. & Huber, R. (1991). *J. Mol. Biol.* **221**, 583–601.

Rydel, T. J., Yin, M., Padmanabhan, K. P., Blankenship, D. T., Cardin, A. D., Correa, P., Fenton, J. W. II & Tulinsky, A. (1994). *J. Biol. Chem.* **269**, 22000–22006.

Scheraga, H. A. (1986). *Ann. NY Acad Sci.* **485**, 124–133.

Skrzypczak-Jankun, E., Carperos, V., Ravichandran, K. G., Tulinsky, A., Westbrook, M. & Maraganore, J. M. (1991). *J. Mol. Biol.* **221**, 1379–1393.

Stubbs, M. T., Oschkinat, H., Mayr, I., Huber, R., Angliker, H., Stone, S. R. & Bode, W. (1992). *Eur. J. Biochem.* **206**, 187–195.

Tulinsky, A. & Qiu, X. (1993). *Blood Coag. Fibrinol.* **4**, 305–312.

Turk, D., Sturzebecher, J. & Bode, W. (1991). *FEBS Lett.* **287**, 133–138.

Vijayalakshmi, J., Padmanabhan, K. P., Mann, K. G. & Tulinsky, A. (1995). *Protein Sci.* In the press.

WITTING, J. I., BOURDON, P., BREZNIAK, D. V., MARAGANORE, J. M. & FENTON, J. W. II (1992). *Biochem. J.* **283**, 737–743.

WU, T. P., YEE, V., TULINSKY, A., CHRUSCIEL, R. A., NAKANISHI, H., SHEN, R., PRIEBE, C. & KAHN, M. (1993). *Protein Eng.* **6**, 471–478.